

RESEARCH ARTICLE | OCTOBER 08 2024

Aging affects the mechanical interaction between microplastics and lipid bilayers

Jean-Baptiste Fleury  ; Vladimir A. Baulin  



J. Chem. Phys. 161, 144902 (2024)

<https://doi.org/10.1063/5.0232678>



Articles You May Be Interested In

Micellar morphological transformations for a series of linear diblock model surfactants

J. Chem. Phys. (March 2014)

Non-monotonous polymer translocation time across corrugated channels: Comparison between Fick-Jacobs approximation and numerical simulations

J. Chem. Phys. (September 2016)

Model microswimmers in channels with varying cross section

J. Chem. Phys. (May 2017)

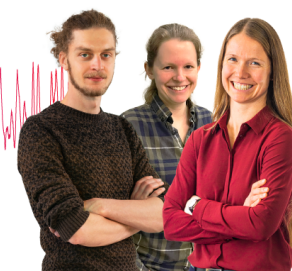
Webinar From Noise to Knowledge

May 13th – Register now



Zurich
Instruments

Universität
Konstanz



Aging affects the mechanical interaction between microplastics and lipid bilayers

Cite as: *J. Chem. Phys.* **161**, 144902 (2024); doi: [10.1063/5.0232678](https://doi.org/10.1063/5.0232678)

Submitted: 9 August 2024 • Accepted: 25 September 2024 •

Published Online: 8 October 2024



View Online



Export Citation



CrossMark

Jean-Baptiste Fleury^{1,a)}  and Vladimir A. Baulin^{2,b)} 

AFFILIATIONS

¹ Universitat des Saarlandes, Experimental Physics and Center for Biophysics, 66123 Saarbruecken, Germany

² Departament d'Enginyeria Quimica, Universitat Rovira i Virgili, Tarragona, Spain

^{a)} E-mail: jean-baptiste.fleury@physik.uni-saarland.de

^{b)} Author to whom correspondence should be addressed: vladimir.baulin@urv.cat

ABSTRACT

Plastic pellets, the pre-production form of many plastic products, undergo oxidation and photodegradation upon exposure to oxygen and sunlight, resulting in visible color changes. This study examines the impact of environmental aging on the mechanical interactions between pellet-derived microplastics and lipid bilayers, a critical component of biological membranes. Polyethylene pellets were collected from La Pineda beach near Tarragona, Spain, and categorized by chemical composition and yellowing index, an indicator of aging. The hydrophilicity of these pellets was assessed using contact angle measurements. Microplastics were produced by grinding and filtering these pellets and subsequently dispersed around a free-standing lipid bilayer within a 3D microfluidic chip to investigate their interactions. Our results reveal that aged microplastics exhibit a significantly increased adhesive interaction with lipid bilayers, leading to greater bilayer stretching. Theoretical modeling indicates a linear relationship between the adhesive interaction and the contact angle of the pellets, reflecting their hydrophilicity. These findings emphasize the increased mechanical impact of aged microplastics on biological membranes, which raises concerns about their potential toxicological effects on living organisms. This study highlights the importance of understanding the interactions between environmentally aged microplastics and biological systems to assess their risks, as these may differ significantly from pristine microplastics often studied under laboratory conditions.

© 2024 Author(s). All article content, except where otherwise noted, is licensed under a Creative Commons Attribution (CC BY) license (<http://creativecommons.org/licenses/by/4.0/>). <https://doi.org/10.1063/5.0232678>

INTRODUCTION

Each year, a considerable amount of plastic accumulates in the oceans, making it one of the major sources of ocean pollution caused by human industrial production.^{1–5} Most thermoplastic materials and products are produced in factories using plastic pellets, also known as pre-production pellets,⁶ which are a significant contributor to ocean pollution.⁷ These plastic materials eventually degrade into microplastics due to wave movement, abrasion, and sun exposure.^{8,9} Microplastics range in size from $\sim 0.1 \mu\text{m}$ to 5 mm^{10,11} and can be carried into the atmosphere by evaporation due to their small size and physical properties.^{12,13} They are then dispersed to other areas when it rains or snows.^{14,15} Microplastics have been found in human organs and blood, raising concerns about the potential and unrecognized risks they pose to human health.^{16–20} Microplastics have been linked to cellular toxicity, tissue inflammation, oxidative stress, membrane damage, and immunological responses through biological or chemical pathways.^{21,22} Recent

studies have aimed to enhance our comprehension of the impact of microplastics on cell-level cytotoxicity, particularly regarding oxidative stress and cell viability. As an example, in vitro evaluations have been conducted using polyethylene (PE) microplastics on two distinct human cell lines: T98G (cerebral cells) and HeLa cells (epithelial cancer cells). The findings from these investigations provide confirmation that oxidative stress is indeed a cellular-level mechanism contributing to cytotoxicity, as evidenced by observations in both cell lines.^{23,24} Recently, it has been reported that microplastics can also mechanically stretch cell membranes through a purely physical mechanism.^{25,26} The results provide evidence that the adsorption of microplastics onto lipid bilayers, including those found in cell membranes, can lead to significant stretching and destabilization of these membranes, as shown in the example of red blood cells (RBCs).²⁵

Pristine microplastics, spherical microparticles created by a chemical reaction, were used in previous studies.^{25,26} Nevertheless, there are notable distinctions between pristine microplastics

and those encountered in the natural environment. Environmental microplastics, as revealed by characterization studies, tend to exhibit irregular shapes and a wide range of sizes. However, the utilization of authentic environmental plastics for risk assessment purposes is frequently impeded by technical and practical obstacles, primarily arising from the heterogeneous nature of the plastics and their diverse size distributions in the environment.^{27,28} Apart from fibers, microplastics in the environment rarely exhibit a spherical shape and are more commonly found to have a grain-like shape.^{27,28} Environmental microplastics are subjected to aging and degradation in addition to shape differences. As a result, these effects may have a significant impact on their surface properties.^{29–31} Microplastics' surface properties are altered by sunlight and photodegradation, which also modifies their hydrophobicity and makes them more likely to adsorb pollutants.^{32–34} These changes in surface properties may alter how they interact with living organisms.³⁵ Many studies have tried to artificially age pristine microplastics to increase the biorelevance of used microplastics.²⁹ However, these techniques seem to present some difficulties in mimicking their environmental alter-ego.²⁹ A recently conducted study introduces a synthesis method that combines different weathering mechanisms to fabricate plastic models with enhanced realism and controllability.³⁶ While the study specifically focuses on polystyrene (PS) material, this approach has the potential to advance risk assessment by enabling more reliable estimations of associated risks.³⁶ These findings hold promise for future studies seeking to enhance the field of risk assessment through improved plastic modeling techniques. Hence, in this investigation, we produced microplastics using plastic pellets sourced from an environmental beach setting. This choice was driven by the composition of the pellets, which predominantly consist of polyethylene (PE), as we will explore in subsequent sections.

Plastic pellets offer several advantages, one of which is that they are usually made from a single plastic component, making their chemical analysis relatively straightforward.^{6,37} Their large size makes it possible to assess their hydrophilicity through contact angle measurements.³⁴ Despite their distinctive shape, they can display varying color changes.³⁸

Plastic aging is intricately linked to the color change of the plastics, known as the yellowing phenomenon. Recent studies, such as the Fourier-transform infrared (FTIR) analysis,³⁹ have studied the chemical modifications underlying the aging process. As plastics age, they undergo oxidation, photodegradation, and thermal degradation, leading to the formation of chromophores like carbonyl and hydroxyl groups. The yellowing of polyethylene is caused by reactions initiated in its structure by ultraviolet (UV) radiation.^{38,40} This change in yellowing index becomes more pronounced with exposure to the environment (age).^{40,41} These chemical changes, detectable through spectroscopic methods, directly correlate with an increase in the yellowing index. Consequently, measuring the yellowing index offers a straightforward method for categorizing plastic pellets based on their age, provided the changes are sufficiently pronounced.

In this study, we utilize plastic pellets to produce microplastics through grinding and filtering the pellets. We then investigate the impact of aging on the physical interaction between microplastics and a model lipid membrane, which is the final barrier that protects cells from the environment. Our results indicate that as the

microplastics age, the bilayer experiences increased stretching due to its enhanced adhesive interaction with the lipid bilayer.

RESULTS AND DISCUSSION

The aging process has a significant impact on the composition and concentration of chemical functional groups present on the surface of microplastics.^{42–44} This factor plays a crucial role in determining the wettability of microplastics in the environment and becomes increasingly important as the size of the microplastics decreases. Figure 1(a) displays a collection of plastic pellets exhibiting various degrees of yellowing.

Initially, our objective was to examine the impact of aging on the surface properties of selected plastic pellets. This was a challenging task as the pellets are large, which renders them susceptible to buoyancy, and not spherical, making it challenging to measure the binding energy at a hydrophilic–hydrophobic interface, as is usually performed with smaller spherical colloids.^{42,43} To address this issue, we determined the contact angle of a sessile water droplet deposited on the surface of one plastic pellet with a quasi-flat surface as observed through microscopic examination. The results of the contact angle Θ measurements, shown in Fig. 1(b), exhibit a large dispersion due to the differences in the topology and surface of the pellets. Our results indicate that the pellets become more hydrophilic as they age, suggesting that the more hydrophilic pellets may have stronger adsorption on the surface of a lipid bilayer.

Next, we investigated the surface properties of the microplastics as a function of the pellets yellowing index. After filtering, we conserve only microplastics that have a diameter of $\approx 1 \mu\text{m}$. We utilized the water pendant method to determine the interfacial tensions at an oil-buffer interface in order to examine the effect of microplastics on a model cell membrane⁴⁵ (see Methods). To evaluate the effect of pellet hydrophilicity on adhesive interactions with a lipid monolayer, we created a buffer droplet in squalene oil containing a phospholipid mixture. This mixture covered the oil-buffer interface and reduced the interfacial tension by forming a lipid monolayer. After adding $\sim 50 \mu\text{g/ml}$ of microplastics to the buffer, as described in the Methods section, we measured the interfacial tension [see Fig. 1(c)], which varied from 1.5 to 2.6 mN/m depending on the pellet Y.I. We used the well-known pendant droplet technique to measure surface tension.⁴⁵ It involves creating a droplet of the liquid sample that hangs from a needle. By analyzing the shape and size of the droplet, we determined the surface tension [as plotted in Fig. 1(c)]. The surface tension is determined by the value of the plateau on the curve, $\approx 2 \text{ mN/m}$ in Fig. 1(c). Subsequently, we present the measurements as a function of microplastics concentration with varying Y.I. [Fig. 1(d)]. Our results confirm that the more hydrophilic the pellet, the stronger the adhesive interaction between the microplastics and the lipid monolayer, as indicated by the yellowing index.

We are now able to calculate the bilayer stress caused by microplastics due to surface tension. To do this, we utilize the same theoretical framework outlined in Ref. 25 applied to mechanical stretching induced by microplastics on a lipid bilayer.

Surface coverage of microplastics is related to the surface concentration of microplastics, and the diameter of the microplastics determines the stretching of the bilayer [see a theoretical model

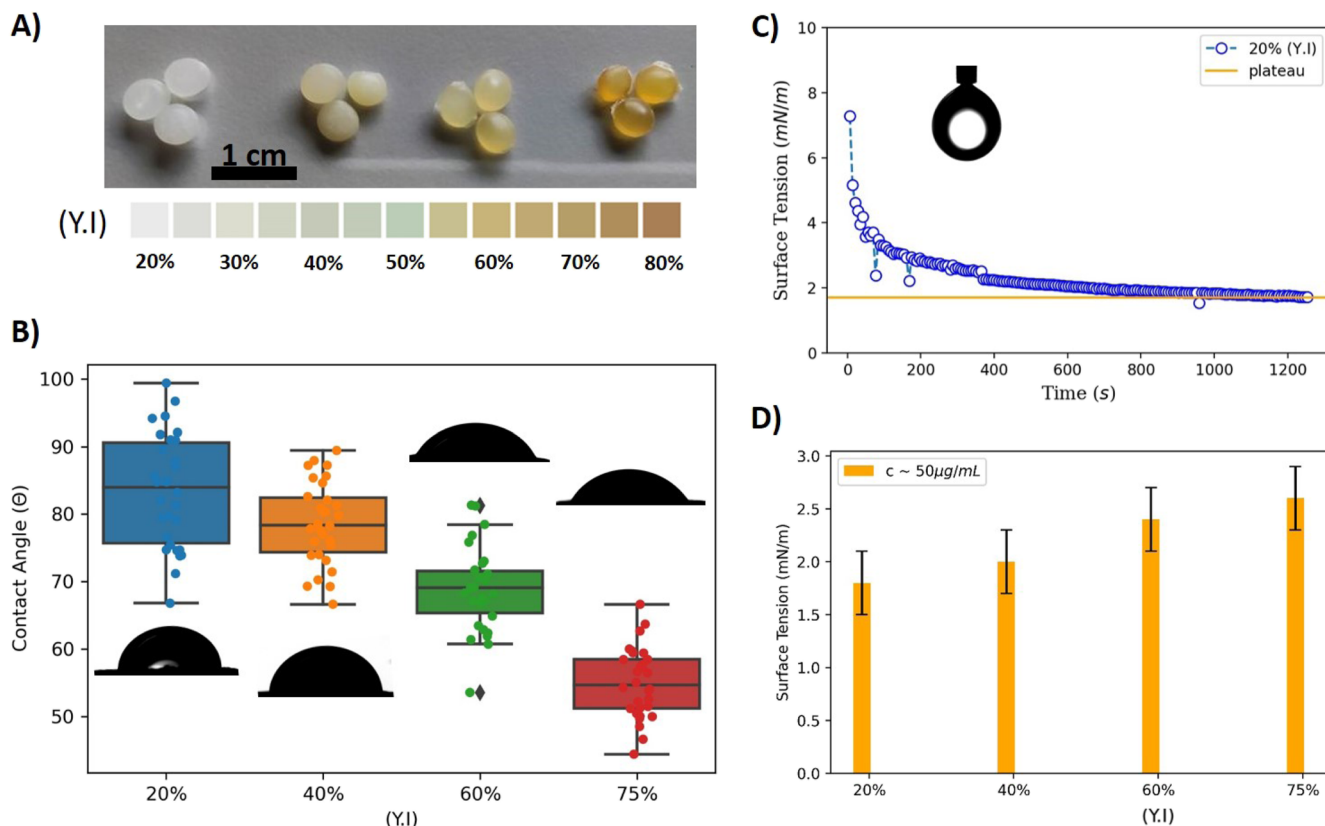


FIG. 1. (a) Photograph of PE pellets classified into four groups based on their yellowing index (Y.I.) with a corresponding color code below, like in the reference. (b) The corresponding contact angle Θ measurements (dots) are presented for a sessile water droplet deposit on a quasi-flat surface of a pellet (with the associated pictures). The yellowing index is used to sort these measurements (for 20%, 40%, 60%, and 75%). (c) One example of surface tension measurement from the water pendant method. The dashed line indicates the surface tension plateau, which is the measured value. The pendant droplet consists of a PBS buffer, and its shape is analyzed as a function of time (s). The buffer droplet was produced in an oily phase (squalene), which contains phospholipids. For this measurement, PE microplastics (from a pellet with a Y.I. $\approx 20\%$) were dispersed in the buffer droplet at a concentration of $50 \mu\text{g/ml}$. (d) Surface tension measurements using the water pendant droplet method (see method section) and a fixed microplastics concentration of $\sim 50 \mu\text{g/ml}$ are plotted with pellets having different Y.I. values.

(Methods)]. To study the effects of yellowing, we established a horizontal bilayer in a 3D microfluidic chip and dispersed microplastics on its surface.⁴⁷ (see Methods). Figure 2(a) shows a microscopic image of a horizontal lipid bilayer in contact with microplastics. The microplastics are represented by black dots or grains, while the lipid bilayer remains invisible under bright field illumination.^{25,47} Our observations via optical microscope showed that microplastics continued to diffuse along the bilayer surface. This diffusion analysis (see methods) allowed us to determine the average diameter of the microplastics ($\approx 1 \mu\text{m}$), which allows us to classify them as individual objects [Fig. 2(b)]. Furthermore, optical microscopy was employed to directly measure the surface coverage of microplastics [see Figs. 2(a) and 2(c)]. Once the surface coverage and size of the microplastics were determined, our subsequent objective was to evaluate the tension of the lipid bilayer.

For this experiment, we fabricated a free-standing lipid bilayer using the Droplet Interface Bilayer (DiB) technique⁴⁸ (see Methods). Figure 3(a) shows an example of a DiB observed by bright-field microscopy. The findings demonstrate that the concentration of

microplastics used directly influences the increase in bilayer tension, and this increase is observed to vary in accordance with the yellowing index of the pellets [see Fig. 3(b)]. For microplastics obtained from pellets with a low Y.I., we observed an increase in bilayer tension (Γ) from 2 to 3 mN/m. The increase in tension was gradual with the rising of the yellowing index of the pellets. For microplastics made of pellets with a high yellowing index, we measured an increase in bilayer tension (Γ) from 2 to 5 mN/m [see Fig. 3(b)].

The model of interaction of pristine microplastics and lipid bilayers with corresponding equations is described in Ref. 25. The details of the calculations for the case of aging are presented in the Methods section. It is remarkable that the interaction parameter ζ , Eq. (2), increases linearly with the measured microplastic contact angle [see Fig. 3(c)]. This finding is consistent with our previous measurements, which showed that the hydrophilicity of microplastics increases with the yellowing index. The resulting interaction parameter ε is depicted as a function of the yellowing index (Y.I.), along with the corresponding linear fit equation: $\varepsilon = -0.0027 - 1.4 \times 10^{-4} (\text{Y.I.})$ [see Fig. 3(c)].

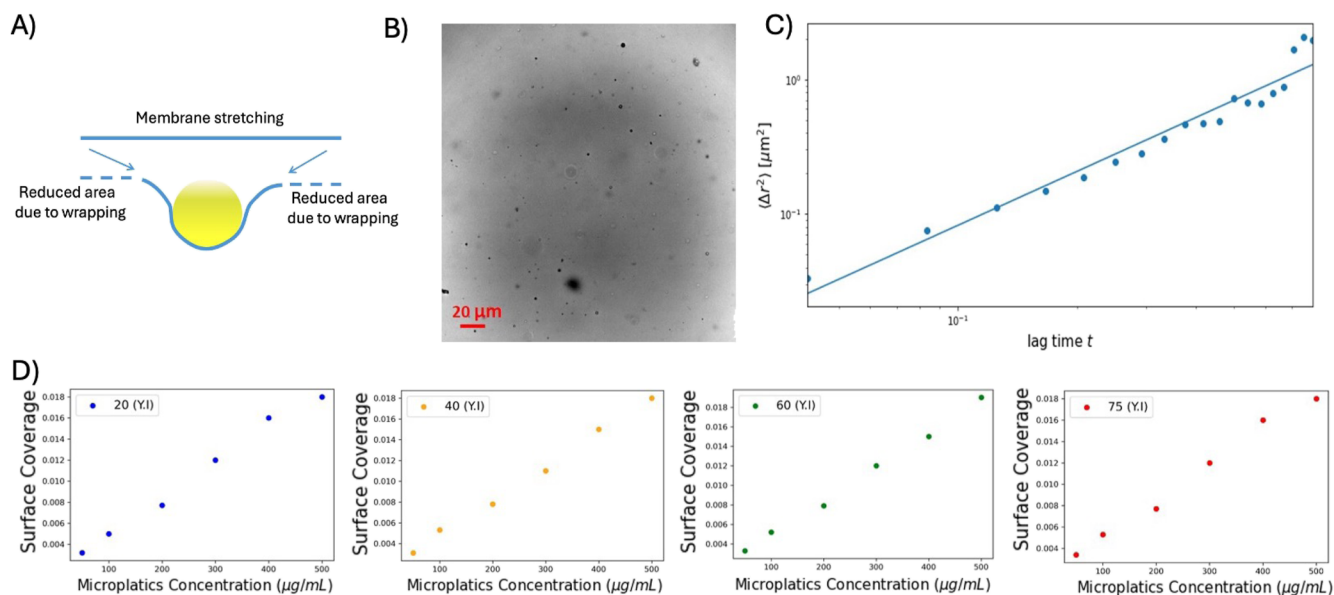


FIG. 2. (a) A mechanism of membrane stretching due to the adsorption of a microplastic at the lipid membrane. (b) A micrograph of microplastics ($c \approx 25 \mu\text{g/ml}$) extracted from a pellet with a Y.I. = 20% at a free-standing lipid bilayer. (c) Mean square displacement ($\langle \Delta r^2 \rangle$) of microplastics at the bilayer as a function of time t in log–log scale. The microplastics' corresponding mean diffusion constant D is equal to $1.7 \mu\text{m}^2/\text{s}$, which corresponds to a spherical particle with a mean diameter of $\approx 1 \mu\text{m}$.⁴⁶ (d) The adsorption isotherm of microplastics adsorbed on a free-standing lipid bilayer as a function of microplastics concentration and Y.I. Each measurement represents an average obtained from 20 different experiments, and the error bar is indicated by the size of the dots.

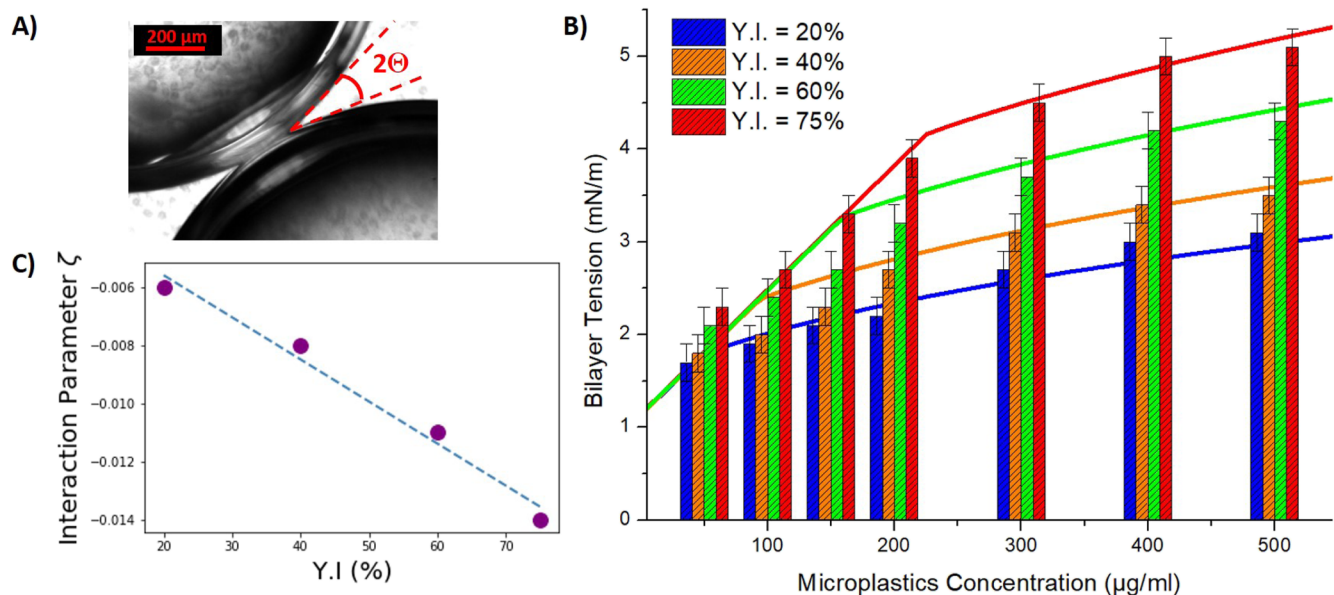


FIG. 3. (a) A microscopic picture of a bilayer formed by the DiB method. The two buffer droplets are made of PBS and contain microplastics ($c \approx 25 \mu\text{g/ml}$). (b) The measured bilayer tensions are displayed as bar graphs, while the theoretical results are shown as continuous lines. We used the surface coverage data from Fig. 2 (b). The measured bilayer tension from the DiB system, obtained from the Young–Dupré equation [Eq.(1)], as a function of different microplastics concentrations and Y.I. The reported bilayer tension values are obtained from an average of 30 measurements, while the continuous line represents the theoretical plot. (c) The resulting interaction parameter ε as a function of Y.I. and the corresponding linear fit $\varepsilon = -0.0027 - 1.4 \times 10^{-4} (\text{Y.I.})$.

According to our theoretical model, the adsorption of each particle onto the bilayer results in a reduction in the total area of the bilayer, which in turn leads to an increase in the membrane tension.²⁵ The physical interaction between microplastics and the bilayer is determined by the adhesion at the contact area. Hence, the more hydrophilic the microplastics are, the stronger their adhesion to the lipid bilayer and the greater the mechanical stretching of the bilayer. Particularly, our fits quantitatively demonstrate that the hydrophilicity of the microplastics linearly increases with the bilayer mechanical stretching.

CONCLUSION

In this study, we investigated how aging affects the physical interaction between polyethylene (PE) microplastics and a lipid bilayer. Both experimental and theoretical methods were employed to demonstrate that the presence of microplastics adsorbed on lipid membranes increases membrane stress, even at low concentrations. The plastic pellets used in this study were collected from La Pineda beach in Spain and were pure polymeric spheres without any additives. The rationale for this is that numerous studies utilize microplastics sourced from suppliers manufactured under controlled laboratory conditions, which may differ substantially from microplastics in the environment.

We isolated plastic pellets consisting solely of PE from the larger population of pellets. The collected plastic pellets from La Pineda beach were subsequently sorted based on their yellowing index, which served as an indicator of their aging state. Contact angle measurements were conducted to assess the hydrophilicity of the pellets, revealing an increase in hydrophilicity corresponding to higher yellowing index values. Subsequently, we obtained micrometer-sized microplastics by grinding and filtering the selected pellets. To investigate the impact of microplastics, we utilized a 3D microfluidic chip to create a self-supporting lipid bilayer and measured its tension in the presence of microplastics.

We demonstrated that the bilayer tension increases linearly with the Y.I. of the pellets, from which the microplastics originate. Particularly, the interaction parameter ζ increases linearly with the measured plastic contact angle. This finding is consistent with our previous measurements,^{25,26} which showed that the hydrophilicity of microplastics increases with the Y.I. Our theoretical model suggests that each adsorbed particle reduces the total area of the bilayer, causing a rise in membrane tension. The physical interaction between microplastics and the bilayer is determined by the adhesion at the contact area. Hence, the more hydrophilic the microplastics are, the stronger their adhesion to the lipid bilayer and the greater the mechanical stretching of the bilayer. Particularly, our fits quantitatively demonstrate that the hydrophilicity of the microplastics increases linearly with the bilayer mechanical stretching. These findings confirm a direct correlation between the hydrophilicity of the microplastics and their adhesion to a lipid bilayer.

Our results provide insight into the mechanisms underlying the interaction between microplastics and lipid bilayers, and the potential effects of aging on this interaction.³⁶ The study builds upon previous research that examined the impact of pristine microplastics on actual biological membranes of red blood cells, as documented in Ref. 25. Therefore, this study brings attention to a need of a more controlled connection between aging, photodegradation, and the

observed effects of microplastics that are found in the environment on living organisms and their difference from pristine microplastics.

METHODS

Molecules

Lipid mixture^{47,49} was obtained by mixing DOPC:DOPE with a molar ratio of 60:40. DOPC is the abbreviation of 1,2-dioleoyl-sn-glycero-3-phosphocholine, DOPE is 1,2-dioleoyl-sn-glycero-3-phosphoethanolamine. All the lipids were purchased from Avanti Polar Lipids (USA). Nile red and all the other chemicals were purchased from Sigma-Aldrich. The buffer phase used in this article is phosphate-buffered saline (PBS) purchased from Sigma-Aldrich. For information, the total ion concentration of PBS solution was $\sim 0.15\text{M}$.

Pellets selection and microplastics production

Environmental microplastics were obtained from plastic pellets manually collected by ONG Good Karma Projects at the beach La Pineda (near Tarragona, Spain). Using the Nile-red staining technique, we characterized the chemical composition of these pellets.^{50,51} It is confirmed, in accordance with Ref. 37, that the predominant composition of the analyzed pellets from this beach is polyethylene (PE). Our study specifically focuses on PE plastics and, therefore, we sort these pellets based on their age. The identification of aged pellets is facilitated by the visible color change from white to yellow, as reported in Ref. 41. The increase in the yellowing index (Y.I.) becomes more pronounced with age and weathering.⁴¹ Consequently, this straightforward technique is employed to categorize the pellets based on their age, given significant changes in Y.I.⁴¹ Alternatively, the combination of the yellowing index with Fourier-transform infrared microscopy is necessary in cases where substantial changes in the yellowing index are not observed. However, in our study, we specifically consider groups of pellets that exhibit a substantial change in Y.I., rendering the use of Fourier-transform infrared microscopy unnecessary.⁴¹ The description of the yellowing index measurement method can be found in one of the subsequent subsections. In order to minimize potential influences arising from surface heterogeneity, we have excluded pellets with cracks from our analysis.⁴¹ Following the sorting of the pellets based on their age, microplastics are generated by grinding these pellets using a grinder⁵² (Torrington, IC20). Subsequently, the microplastics are subjected to size separation using filters to retain only those with an approximate size of $1\ \mu\text{m}$.⁴¹ To achieve this objective, we initially pass the buffer through a primary sieve with a pore size of $10\ \mu\text{m}$ (pluriStrainer obtained from pluriSelect, Germany). Subsequently, the buffer is passed through a HPLC syringe filter (filter number 7-8808, Neolab) with a pore size ranging from 1 to $2\ \mu\text{m}$. We use the concentration of microplastics $50\ \mu\text{g}/\text{ml}$ to be consistent with the range of concentrations in Ref. 25.

Upon the production of microplastics, their morphologies were examined using optical microscopy. The microplastics exhibited a wide range of shapes, which could be easily quantified for sizes spanning from 10 to $100\ \mu\text{m}$. We analyze the shape distribution of microplastics within this range because it is sufficiently large to be characterized using fluorescent microscopy. However, for the purpose of this study, our focus lies on microplastics in the micrometer

range, as they exhibit a similar distribution of shapes as described by Allen *et al.*³⁸ Microplastics of this size enable substantial coverage of the bilayer surface by a significant number of particles, thereby minimizing the influence of shape heterogeneity on the interaction between microplastics and the bilayer.

These formed microplastics stay spontaneously at the bilayer surface after insertion inside the microfluidic chip from the bottom channel. Interestingly, they do not aggregate on the bilayer surface, as demonstrated by optical microscopy. Due to their slight hydrophobicity, their zeta potential cannot be measured with a standard technique.

Surface tension measurements

The surface tension of various lipid monolayers at the oil-buffer interface was obtained by the pendant drop method using a commercial measurement device (OCA 20, DataPhysics Instruments GmbH, Filderstadt, Germany). An oil solution containing 5 mg/ml lipids was produced by introducing a droplet from a steel needle into the surrounding oil phase. The interfacial tension was obtained from the automatically fitting of the shapes of the droplets by the Young–Laplace equation (OCA 20 does it automatically).^{45,53} To increase the statistics, we conducted 30 additional measurements by the Y.I. and determined an acceptable average contact angle.

Determination of the yellowing index

The Yellowing Index (Y.I.) of plastic pellets was quantified using coordinates in a three-dimensional color-space diagram [see Fig. 1 (Sec. II C) of Ref. 41]. This system allows the brightness or luminosity of a color to be quantified; the color varies from black to white, with values from 0 to 100. This extremely detailed method allows for an easy and reproducible measurement of the Y.I.⁴¹

Diffusion analysis

To determine the average particle radius, from the diffusion analysis, we calculate the mean square displacement. The Mean Square Displacement (MSD), denoted as $\langle r(t)^2 \rangle$, is obtained by tracking the positions r of particles at different time points and calculating the squared displacement between each position and its initial position. These squared displacements are then averaged over all particles to obtain the MSD value,

$$\langle r(t)^2 \rangle = \frac{1}{N} \sum [\mathbf{r}(t + \Delta t) - \mathbf{r}(t)]^2,$$

where N is the total number of particles and Δt is the time interval. For a spherical particle, the average radius R can be obtained from the Stokes–Einstein equation:

$$R = \frac{k \cdot T}{6\pi\eta D},$$

where $D = \langle r(t)^2 \rangle / 4t$. This equation establishes the relationship between the average radius R , Boltzmann constant k , absolute temperature T , dynamic viscosity η , and the diffusion coefficient D . References 54 and 55 provide further details on these concepts. Additionally, detailed explanations of the image analysis can be found in Refs. 25 and 56.

Droplet interface bilayer

A lipid mixture^{47,49} was obtained by mixing DOPC:DOPE with a molar ratio of 60:40. The lipids were dissolved using squalene oil at a concentration of 5 mg/ml. Using magnetic stirring, the lipids were maintained at 50 °C for 24 h. A glass cylinder that has a 7 cm diameter and a 1 cm height and is coated with OTS (see Ref. 25) was filled with the oil–lipid mixture. A significant amount of the cylinder area can be observed with a Leica Z16 microscope and a PCO1600 camera. It is enough to observe the formation of DiB (Droplet interface Bilayer). To form DiB, we produced a microdroplet with a micropipette that has a tip and a typical diameter of 1 mm, which was made using a micropipette puller (Eppendorf). Using this method, two water droplets of about equal size are manually produced in the container and left there for 30 minutes. They were delicately brought together using a needle. At the point where two droplets interact, a bilayer spontaneously forms within a brief period of time.^{25,48,57} Each droplet's content contains a controlled quantity of microplastic that was dissolved into the buffer prior to droplet production. Optical confirmation of the bilayer was performed using a microscope, and the bilayer tension Γ was determined using the Young–Dupré law,^{45,57}

$$\Gamma = 2\gamma \cos(\theta), \quad (1)$$

where 2θ is the contact angle of the bilayer and γ is the interfacial tension.^{45,57}

Microfluidic 3D device

A 3D microfluidic device was used to produce a horizontal bilayer. 3D printing was used to make two molds from a block of polydimethylsiloxane (PDMS) (Sylgard 184, Dow Corning).⁴⁷ The PDMS block was plasma-bound to a glass coverslip following plasma treatment (Diener). The following sources, including Refs. 25, 47, 58, and 59, provide a detailed description of this technique. The chip was then filled entirely with an oil–lipid mixture. The lipids were dissolved using squalene oil at a concentration of 5 mg/ml. The two buffer phases were then injected face-to-face until they came together in the desired location. Each water–oil interface was covered by a lipid monolayer; when two monolayers came into contact, they fused to form a lipid bilayer.^{25,47,58,59}

Theoretical modeling

This model outlines the localized distortion of the lipid bilayer caused by the adsorption of microplastics and the subsequent mechanical stretching of the lipid bilayer. A similar model was used to evaluate the effect of nanopillars on the stretching of cell membranes⁶⁰ and to mechanically deform bacteria cell membranes with gold nanoparticles.⁶¹ In this model, the area per microplastic particle is divided into two parts: the “suspended” and the “adsorbed” layers. The balance between the stretching and compression of the two layers and the attraction of the microplastics in the contact region determines the equilibrium position of the layer. When particles are adsorbed onto the membrane, the “suspended” layer is stretched to increase contact between the membrane and the particle in the suspended layer. As a result, the energy of the membrane is the sum of the energy gained through adsorption in the adsorbed layer and

the stretching of the membrane in the suspended layer. Within this model, the mechanical stretching is controlled by the ratio,

$$\zeta = \frac{\epsilon n_0}{k}, \quad (2)$$

where ϵn_0 is the attractive interaction energy per area. The adhesion energies of microplastics, as estimated from experimental measurements, are on the order of 1 mJ/m^2 ,^{62,63} while the compressibility constant of a lipid bilayer is $k \sim 100 - 300 \text{ mN/m}$. The control interaction parameter ζ is estimated to range from -0.003 to -0.01 for bare plastics. Although this model is typically based on spherical objects, our results indicate that it is still valid even when using grain-like shaped objects with micrometer-sized dimensions. This size is appropriate because it allows for a large coverage of the bilayer surface by microplastics, effectively averaging out any differences in shape in terms of their interactions.

ACKNOWLEDGMENTS

VAB acknowledges financial assistance from the Ministerio de Ciencia, Innovación y Universidades of the Spanish Government through research Project No. PID2020-114347RB-C33, financed by MCIN/AEI 10.13039/501100011033. The authors are grateful to the Good Karma Projects (ONG) for collecting and providing microplastic pellets.

AUTHOR DECLARATIONS

Conflict of Interest

The authors have no conflicts to disclose.

Author Contributions

Jean-Baptiste Fleury: Conceptualization (equal); Data curation (equal); Formal analysis (equal); Investigation (equal); Methodology (equal); Resources (equal); Validation (equal); Visualization (equal); Writing – original draft (equal). **Vladimir A. Baulin:** Conceptualization (equal); Data curation (equal); Formal analysis (equal); Funding acquisition (equal); Investigation (equal); Methodology (equal); Validation (equal); Visualization (equal); Writing – original draft (equal).

DATA AVAILABILITY

The data that support the findings of this study are available from the corresponding author upon reasonable request.

REFERENCES

- J. A. Brandon, W. Jones, and M. D. Ohman, "Multidecadal increase in plastic particles in coastal ocean sediments," *Sci. Adv.* **5**, eaax0587 (2019).
- K. Pabortsava and R. S. Lampitt, "High concentrations of plastic hidden beneath the surface of the Atlantic Ocean," *Nat. Commun.* **11**, 4073 (2020).
- S. Morét-Ferguson, K. L. Law, G. Proskurowski, E. K. Murphy, E. E. Peacock, and C. M. Reddy, "The size, mass, and composition of plastic debris in the western north Atlantic ocean," *Mar. Pollut. Bull.* **60**, 1873–1878 (2010).

- A. T. Pruter, "Sources, quantities and distribution of persistent plastics in the marine environment," *Mar. Pollut. Bull.* **18**, 305–310 (1987).
- X. Guo and J. Wang, "The chemical behaviors of microplastics in marine environment: A review," *Mar. Pollut. Bull.* **142**, 1–14 (2019).
- T. M. Karlsson, L. Arneborg, G. Broström, B. C. Almroth, L. Gipperth, and M. Hassellöv, "The unaccountability case of plastic pellet pollution," *Mar. Pollut. Bull.* **129**, 52–60 (2018).
- B. G. Yeo, H. Takada, J. Hosoda, A. Kondo, R. Yamashita, M. Saha, and T. Maes, "Polycyclic aromatic hydrocarbons (PAHs) and hopanes in plastic resin pellets as markers of oil pollution via international pellet watch monitoring," *Arch. Environ. Contam. Toxicol.* **73**, 196–206 (2017).
- K. Zhang, A. H. Hamidian, A. Tubić, Y. Zhang, J. K. H. Fang, C. Wu, and P. K. S. Lam, "Understanding plastic degradation and microplastic formation in the environment: A review," *Environ. Pollut.* **274**, 116554 (2021).
- L. Sørensen, A. S. Groven, I. A. Hovsbakken, O. Del Puerto, D. F. Krause, A. Sarno, and A. M. Booth, "UV degradation of natural and synthetic microfibers causes fragmentation and release of polymer degradation products and chemical additives," *Sci. Total Environ.* **755**, 143170 (2021).
- A. Haegerbaeumer, M.-T. Mueller, H. Fueser, and W. Traunspurger, "Impacts of micro- and nano-sized plastic particles on benthic invertebrates: A literature review and gap analysis," *Front. Environ. Sci.* **7**, 17 (2019).
- G. Erni-Cassola, V. Zadjelovic, M. I. Gibson, and J. A. Christie-Oleza, "Distribution of plastic polymer types in the marine environment; A meta-analysis," *J. Hazard. Mater.* **369**, 691–698 (2019).
- M. C. Rillig, "Microplastic in terrestrial ecosystems and the soil?," *Environ. Sci. Technol.* **46**, 6453–6454 (2012).
- S. Allen, D. Allen, K. Moss, G. Le Roux, V. R. Phoenix, and J. E. Sonke, "Examination of the ocean as a source for atmospheric microplastics," *PLoS One* **15**, e0232746 (2020).
- W. Xia, Q. Rao, X. Deng, J. Chen, and P. Xie, "Rainfall is a significant environmental factor of microplastic pollution in inland waters," *Sci. Total Environ.* **732**, 139065 (2020).
- M. Bergmann, S. Mützel, S. Primpke, M. B. Tekman, J. Trachsel, and G. Gerdtts, "White and wonderful? Microplastics prevail in snow from the alps to the arctic," *Sci. Adv.* **5**, eaax1157 (2019).
- A. D. Vethaak and J. Legler, "Microplastics and human health," *Science* **371**, 672–674 (2021).
- S. L. Wright and F. J. Kelly, "Plastic and human health: A micro issue?," *Environ. Sci. Technol.* **51**, 6634–6647 (2017).
- B. Li, L. Su, H. Zhang, H. Deng, Q. Chen, and H. Shi, "Microplastics in fishes and their living environments surrounding a plastic production area," *Sci. Total Environ.* **727**, 138662 (2020).
- J. A. Gil-Delgado, D. Guijarro, R. U. Gosálvez, G. M. López-Iborra, A. Ponz, and A. Velasco, "Presence of plastic particles in waterbirds faeces collected in Spanish lakes," *Environ. Pollut.* **220**, 732–736 (2017).
- S. Wagner and T. Reemtsma, "Things we know and don't know about nanoplastic in the environment," *Nat. Nanotechnol.* **14**, 300–301 (2019).
- A. Banerjee and W. L. Shelver, "Micro- and nanoplastic induced cellular toxicity in mammals: A review," *Sci. Total Environ.* **755**, 142518 (2021).
- M. Hu and D. Palić, "Micro- and nano-plastics activation of oxidative and inflammatory adverse outcome pathways," *Redox Biol.* **37**, 101620 (2020).
- G. F. Schirinzì, I. Pérez-Pomeda, J. Sanchís, C. Rossini, M. Farré, and D. Barceló, "Cytotoxic effects of commonly used nanomaterials and microplastics on cerebral and epithelial human cells," *Environ. Res.* **159**, 579–587 (2017).
- C. Campanale, C. Massarelli, I. Savino, V. Locaputo, and V. F. Uricchio, "A detailed review study on potential effects of microplastics and additives of concern on human health," *Int. J. Environ. Res. Public Health* **17**, 1212 (2020).
- J.-B. Fleury and V. A. Baulin, "Microplastics destabilize lipid membranes by mechanical stretching," *Proc. Natl. Acad. Sci. U. S. A.* **118**, e2104610118 (2021).
- J. B. Fleury and V. A. Baulin, "Synergistic effects of marine pollutants and microplastics on the destabilization of lipid bilayers," *J. Phys. Chem. B* **128**(36), 8753–8761 (2024).
- S. Kefer, O. Miesbauer, and H.-C. Langowski, "Environmental microplastic particles vs. Engineered plastic microparticles—A comparative review," *Polymers* **13**, 2881 (2021).

- ²⁸A. E. Rubin, A. K. Sarkar, and I. Zucker, "Questioning the suitability of available microplastics models for risk assessment – A critical review," *Sci. Total Environ.* **788**, 147670 (2021).
- ²⁹O. S. Alimi, D. Claveau-Mallet, R. S. Kurusu, M. Lapointe, S. Bayen, and N. Tufenkji, "Weathering pathways and protocols for environmentally relevant microplastics and nanoplastics: What are we missing?," *J. Hazard. Mater.* **423**, 126955 (2022).
- ³⁰J. N. Hanun, F. Hassan, and J.-J. Jiang, "Occurrence, fate, and sorption behavior of contaminants of emerging concern to microplastics: Influence of the weathering/aging process," *J. Environ. Chem. Eng.* **9**, 106290 (2021).
- ³¹K. Bhagat, A. C. Barrios, K. Rajwade, A. Kumar, J. Oswald, O. Apul, and F. Perreault, "Aging of microplastics increases their adsorption affinity towards organic contaminants," *Chemosphere* **298**, 134238 (2022).
- ³²S. H. Joo, Y. Liang, M. Kim, J. Byun, and H. Choi, "Microplastics with adsorbed contaminants: Mechanisms and treatment," *Environ. Challenges* **3**, 100042 (2021).
- ³³G. Binda, G. Zanetti, A. Bellasi, D. Spanu, G. Boldrocchi, R. Bettinetti, A. Pozzi, and L. Nizzetto, "Physicochemical and biological ageing processes of (micro)plastics in the environment: A multi-tiered study on polyethylene," *Environ. Sci. Pollut. Res.* **30**, 6298 (2022).
- ³⁴A. Al Harraq and B. Bharti, "Microplastics through the lens of colloid science," *ACS Environ. Au* **2**, 3–10 (2022).
- ³⁵O. Missawi, N. Bousserrhine, N. Zitouni, M. Maisano, I. Boughattas, G. De Marco, T. Cappello, S. Belbekhouche, M. Guerrouache, V. Alphonse, and M. Banni, "Uptake, accumulation and associated cellular alterations of environmental samples of microplastics in the seaworm *Hediste diversicolor*," *J. Hazard. Mater.* **406**, 124287 (2021).
- ³⁶A. K. Sarkar, A. E. Rubin, and I. Zucker, "Engineered polystyrene-based microplastics of high environmental relevance," *Environ. Sci. Technol.* **55**, 10491–10501 (2021).
- ³⁷N. Expósito, J. Rovira, J. Sierra, J. Folch, and M. Schuhmacher, "Microplastics levels, size, morphology and composition in marine water, sediments and sand beaches. Case study of Tarragona coast (western Mediterranean)," *Sci. Total Environ.* **786**, 147453 (2021).
- ³⁸N. S. Allen, M. Edge, and S. Hussain, "Perspectives on yellowing in the degradation of polymer materials: Inter-relationship of structure, mechanisms and modes of stabilisation," *Polym. Degrad. Stab.* **201**, 109977 (2022).
- ³⁹C. Campanale, I. Savino, C. Massarelli, and V. F. Uricchio, "Fourier transform infrared spectroscopy to assess the degree of alteration of artificially aged and environmentally weathered microplastics," *Polymers* **15**, 911 (2023).
- ⁴⁰M. M. Elmer-Dixon, L. P. Fawcett, B. R. Hinderliter, and M. A. Maurer-Jones, "Could superficial chiral nanostructures be the reason polyethylene yellows as it ages?," *ACS Appl. Polym. Mater.* **4**, 6458–6465 (2022).
- ⁴¹B. Abaroa-Pérez, S. Ortiz-Montosa, J. J. Hernández-Brito, D. Vega-Moreno, and D. Yellowing, "Yellowing, weathering and degradation of marine pellets and their influence on the adsorption of chemical pollutants," *Polymers* **14**, 1305 (2022).
- ⁴²A. Al Harraq, P. J. Brahana, O. Arcemont, D. Zhang, K. T. Valsaraj, and B. Bharti, "Effects of weathering on microplastic dispersibility and pollutant uptake capacity," *ACS Environ. Au* **2**, 549–555 (2022).
- ⁴³J. G. Lee, L. L. Larive, K. T. Valsaraj, and B. Bharti, "Binding of lignin nanoparticles at oil–water interfaces: An ecofriendly alternative to oil spill recovery," *ACS Appl. Mater. Interfaces* **10**, 43282–43289 (2018).
- ⁴⁴X. Hua, M. A. Bevan, and J. Frechette, "Competitive adsorption between nanoparticles and surface active ions for the oil–water interface," *Langmuir* **34**, 4830–4842 (2018).
- ⁴⁵J. Bibette, F. L. Calderon, and P. Poulin, "Emulsions: Basic principles," *Rep. Prog. Phys.* **62**, 969–1033 (1999).
- ⁴⁶X. Bian, C. Kim, and G. E. Karniadakis, "111 years of Brownian motion," *Soft Matter* **12**, 6331–6346 (2016).
- ⁴⁷P. Heo, S. Ramakrishnan, J. Coleman, J. E. Rothman, J.-B. Fleury, and F. Pincet, "Highly reproducible physiological asymmetric membrane with freely diffusing embedded proteins in a 3D-printed microfluidic setup," *Small* **15**, 1900725 (2019).
- ⁴⁸H. Bayley, B. Cronin, A. Heron, M. A. Holden, W. L. Hwang, R. Syeda, J. Thompson, and M. Wallace, "Droplet interface bilayers," *Mol. BioSyst.* **4**, 1191–1208 (2008).
- ⁴⁹G. van Meer, D. R. Voelker, and G. W. Feigenson, "Membrane lipids: Where they are and how they behave," *Nat. Rev. Mol. Cell Biol.* **9**, 112–124 (2008).
- ⁵⁰T. Maes, R. Jessop, N. Wellner, K. Haupt, and A. G. Mayes, "A rapid-screening approach to detect and quantify microplastics based on fluorescent tagging with Nile Red," *Sci. Rep.* **7**, 44501 (2017).
- ⁵¹N. Meyers, A. I. Catarino, A. M. Declercq, A. Brenan, L. Devriese, M. Vandegheuchte, B. De Witte, C. Janssen, and G. Everaert, "Microplastic detection and identification by Nile red staining: Towards a semi-automated, cost- and time-effective technique," *Sci. Total Environ.* **823**, 153441 (2022).
- ⁵²M. Völkl, V. Jérôme, A. Weig, J. Jasinski, N. Meides, P. Stroehriegl, T. Scheibel, and R. Freitag, "Pristine and artificially-aged polystyrene microplastic particles differ in regard to cellular response," *J. Hazard. Mater.* **435**, 128955 (2022).
- ⁵³Y. Guo, M. Werner, R. Seemann, V. A. Baulin, and J.-B. Fleury, "Tension-induced translocation of an ultrashort carbon nanotube through a phospholipid bilayer," *ACS Nano* **12**, 12042–12049 (2018).
- ⁵⁴H. A. Kramers, "Brownian motion in a field of force and the diffusion model of chemical reactions," *Physica* **7**, 284–304 (1940).
- ⁵⁵P. Hänggi, P. Talkner, and M. Borkovec, "Reaction-rate theory: Fifty years after kramers," *Rev. Mod. Phys.* **62**, 251–341 (1990).
- ⁵⁶J.-B. Fleury, V. A. Baulin, and X. Le Guével, "Protein-coated nanoparticles exhibit Lévy flights on a suspended lipid bilayer," *Nanoscale* **14**, 13178–13186 (2022).
- ⁵⁷J.-B. Fleury, "Enhanced water permeability across a physiological droplet interface bilayer doped with fullerenes," *RSC Adv.* **10**, 19686–19692 (2020).
- ⁵⁸S. Puza, S. Caesar, C. Poojari, M. Jung, R. Seemann, J. S. Hub, B. Schrul, and J.-B. Fleury, "Lipid droplets embedded in a model cell membrane create a phospholipid diffusion barrier," *Small* **18**, e2106524 (2022).
- ⁵⁹J.-B. Fleury, M. Werner, X. L. Guével, and V. A. Baulin, "Protein corona modulates interaction of spiky nanoparticles with lipid bilayers," *J. Colloid Interface Sci.* **603**, 550–558 (2021).
- ⁶⁰S. Pogodin, J. Hasan, V. A. Baulin, H. K. Webb, V. K. Truong, T. Phong Nguyen, V. Boshkovikj, C. J. Fluke, G. S. Watson, J. A. Watson, R. J. Crawford, and E. P. Ivanova, "Biophysical model of bacterial cell interactions with nanopatterned cicada wing surfaces," *Biophys. J.* **104**, 835–840 (2013).
- ⁶¹D. P. Linklater, V. A. Baulin, S. Juodkakis, R. J. Crawford, P. Stoodley, and E. P. Ivanova, "Mechano-bactericidal actions of nanostructured surfaces," *Nat. Rev. Microbiol.* **19**, 8–22 (2021).
- ⁶²M. Deserno and W. M. Gelbart, "Adhesion and wrapping in colloid–vesicle complexes," *J. Phys. Chem. B* **106**, 5543–5552 (2002).
- ⁶³C. Dietrich, M. Angelova, and B. Pouligny, "Adhesion of latex spheres to giant phospholipid vesicles: Statics and dynamics," *J. Phys. II France* **7**, 1651–1682 (1997).